Formation of Moderate-Size Bubbles

JOHN F. MAHONEY, JR., and LEONARD A. WENZEL

Lehigh University, Bethlehem, Pennsylvania

Bubbles were formed in water when air was passed through a single square-edged orifice which had been drilled in a glass plate. The glass plate was 0.05 in. thick, and the orifice diameter was ⅛ in. The air chambers above the liquid surface and below the orifice plate were varied. The extreme values of these volumes were 0.00975 and 0.195 cu. ft. The air rate through the orifice, Q was as great as 200×10^{-5} cu. ft./sec. Bubble frequencies, f, were as great as 16 $sec.^{-1}$

Both the upper and lower chamber volume influenced markedly the relationship between f and Q. A relationship that predicts sets of upper and lower chamber volumes that result in the same f vs. Q relation is given. A two-parameter equation that gives f as a function of Q is presented.

Wettability of the orifice plate and the liquid depth over the orifice plate were also considered as independent variables.

The factors controlling bubble formation from single submerged orifices have been considered frequently (*1* to *6, 10, 12*). Figure 1 shows schematically three types of bubblers that are considered. Although the type 2 bubbler more nearly simulates that which is found in mass transfer applications, it has received less theoretical attention than the type 1 bubbler. Hitherto, the type 3 bubbler has not been treated at all. This paper shows the relationship between these bubbler types and explores the mechanics of bubble formation.

At one time it was supposed that the volume of a bubble formed from a type 1 bubbler could be calculated from a force balance of the form

$$v(\rho_L - \rho_G)g = d\pi\sigma \qquad (1)$$

If this equation is correct, v/d should be a constant for a given system since it involves only constants and system properties. For the air-water system v/d is 0.231 sq. cm. Benzing and Meyers (*1*) found that experimental-literature values varied between 0.04 and 1.0 for this system.

Hughes, et al. (*5*) pointed out that the reason for this discrepancy was probably a failure to appreciate the effect of V_L, the volume of the chamber upstream from the orifice. They wrote a complete force balance around the forming bubble in a type 1 bubbler and, in solution, simplified it by assuming gas momentum to be negligible. From this solution an electrical analogue resulted in which the lower chamber gas volume was simulated by a capacitor and the fluid friction and inertia by a resistor and inductor. Davidson and Amick (*4*) showed qualitatively the relation between V_L and the bubble formation frequency, f; decreasing V_L increased f.

DESCRIPTION OF APPARATUS

The apparatus is shown schematically in Figure 2. The vertical walls of the apparatus were made of 5 inch O.D. and 3/16 inch thick lucite cylinder. The orifice plate was a piece of glass 0.05 inch thick with a ⅛ inch hole drilled in its center. Glass was used so that its wetting properties could be varied by proper treatment. When the orifice plate was cleaned, it had a contact angle of about 30 deg. Upon treatment with dimethyldichlorosilane, the contact angle became 90 deg. The two chamber volumes, V_U and V_L, were varied by using different lengths of lucite tubing. To obtain $V_L = \infty$ or $V_U = \infty$, the apparatus was modified. In the case of a type 1 or 2 bubbler, the gas used was cylinder air. In the type 3 bubbler atmospheric air was induced to flow through the apparatus with an aspirator. Air flow rates were measured with a wet-test meter. Since pressure drop through the apparatus was small, no pressure correction was made to the wet-test meter readings. A 6 inch depth of water stood on the plate in most of the work, but variation of water height from 2⅝ inch to 12½ inch had no effect on the bubble-formation frequency.

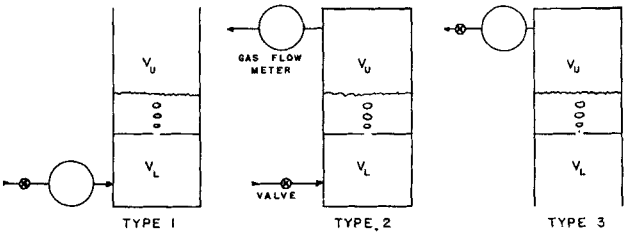

Fig. 1. Schematic diagram of bubble types.

The frequency of bubble formation was found by measuring the number of times a light beam was interrupted. A narrow beam of light was passed horizontally over the orifice. When no bubble interfered, the light struck a photo tube. The output of the tube went to a high-speed recorder. The frequency could then be calculated by counting the blips per unit length of the recorder tape. Figure 3(A) shows a typical tape.

High-speed motion pictures of the orifice in action were also used. These were taken with a camera placed about 2 ft. from the orifice. Film speeds of 2,000 to 4,000 frames/sec. gave adequate resolution of the bubbling action. These films were analyzed to obtain bubble-formation times and were useful in a qualitative understanding of the bubbling phenomenon.

DATA AND OBSERVATIONS

Data of bubble frequency, f, and weep rate, w, were taken over a range of gas flow rates. Parameters were up-

J. F. Mahoney is with West Virginia University, Morgantown, West Virginia.

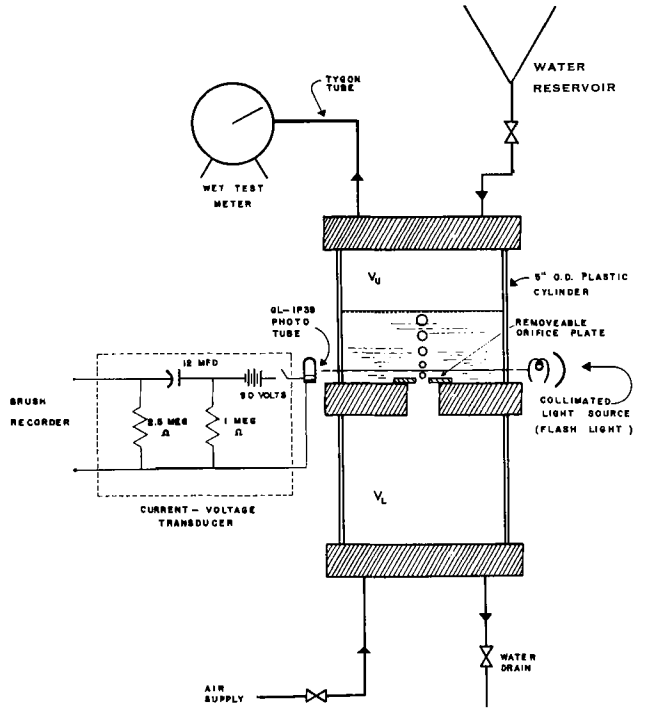

Fig. 2. Experimental apparatus for bubble-frequency measurement.

per and lower chamber volumes, plate wettability, and liquid depth over the orifice. The data discussed here were selected for their bearing on bubble-formation mechanism. Reference 8 presents the complete data.

Figure 4 presents the variation of bubble frequency with gas volumetric flow rate for several sets of upper and lower chamber volumes. These data were obtained with a 6 in. liquid depth over a nonwet orifice plate. On this figure curve B represents data obtained from several pairs of upper and lower chamber volumes. The first of these sets ($V_U = 0.159$ cu. ft., $V_L = 0.122$ cu ft.) was chosen at random. The other two sets were found by changing V_L and then varying V_U until the identical frequency curve was obtained. Several such sets of data were obtained. This implies that a family of frequency curves exists, each of which will result from an infinite number of sets of V_U and V_L. Curve A in Figure 4 was produced when one of the sets that made up curve B (points given by circles) was taken and the value of V_U decreased. The reduction in V_U displaced the frequency curve upward. This inverse relation between V_U and f is qualitatively the same as the relation between V_L and f observed by Davidson and Amick (4).

Curve A also serves to illustrate the peculiar phenomenon called *cluster formation*. If V_U (and/or V_L) is sufficiently small, and for small values of the time averaged volumetric flow rate, Q, bubbles form in a more complicated periodic pattern, that is, in clusters. The situation

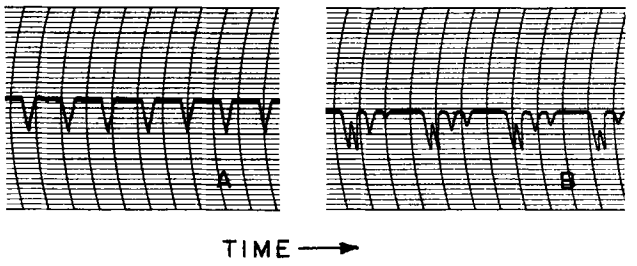

Fig. 3. Recorder traces of bubble passage. (A) Single bubbles being formed (B) Cluster formation of bubbles occurring.

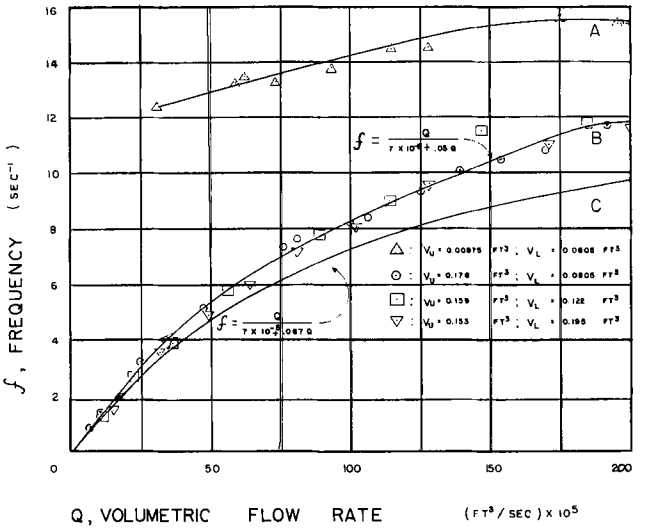

Fig. 4. Bubble frequency as influenced by gas flow rate and gas chamber volumes. The contact angle is 90 deg.

is described best by the recorder trace given in Figure 3(B). Newer members of a cluster have progressively smaller volumes as may be discerned qualitatively. It is for this reason that the first part of curve A in Figure 4 is missing. Bubble frequency becomes ambiguous when cluster formation is present. Although cluster formation is interesting, any frequency curve that showed signs of it was excluded from the discussions because of the complexities introduced.

The growth time, T, was measured with a camera. This quantity represents the length of time that air passed through the orifice into a single bubble. The surprising results are shown in Figure 5 where growth time is plotted against Q. Growth time does not vary with Q. In Figure 5 the values of V_U and V_L were the same as those used to obtain some of the points of curve B of Figure 4. The formation time was not noticeably longer when Q (or f) was made arbitrarily small. Even in the case of a value of Q so small that only one bubble formed per minute, the formation time was still not noticeably increased. The orifice remained quiescent during most of the cycle ($1/f$ sec.) except for a short period of bubble growth (T). This observation indicates that, in the range of variables used, the surface tension-buoyant force model of bubble formation is inadequate.

THEORY AND ANALYSIS OF RESULTS

The observations presented point to a mechanism of bubble formation different from that previously developed. After enough air is added to the lower chamber (or removed from the upper chamber), a critical pressure dif-

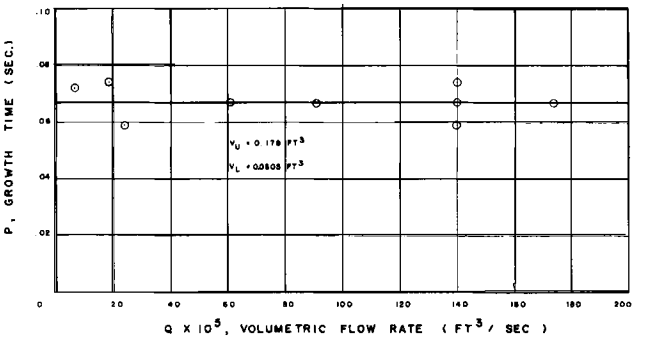

Fig. 5. Measured bubble-growth time as a function of gas flow rate with fixed chamber volumes.

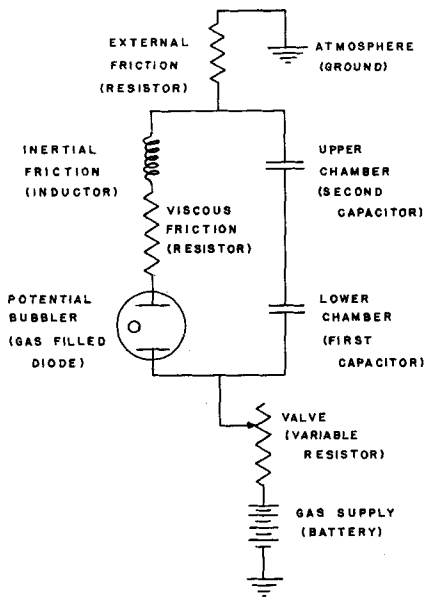

Fig. 6. Electrical analogue of bubble formation mechanism.

ference between the upper and lower chamber is achieved. At this time a bubble starts to form. If this pressure potential is less than the critical starting value, there is no evidence of bubble formation. Furthermore, it is asssumed that bubble formation after having started, continues until a critical stopping potential is reached. Moreover both starting and stopping potentials are assumed to be independent of Q (or of any other rate). This mechanism might be called *potential bubble formation.*

According to Hughes (5) the upper and lower chambers act as linear energy storing devices and hence may be represented in an analogue by capacitors. In such an analogue the notion of potential bubble formation is carried over by the use of a gas-filled diode. The diode does not pass current unless a certain critical starting potential (voltage this time) is achieved. The tube continues to function until the potential drops below the critical stopping potential. Friction and inertia in gas flow through the orifice are represented in such an analogue by resistors and inductors, respectively.

The analogue is shown in Figure 6. A molecule of air (electron) is taken from the supply tank (battery) and reduced in pressure (voltage) by a valve (resistor). It is then passed into the lower chamber (first capacitor) where it is stored until the pressure (voltage) becomes great enough to initiate bubble formation (tube firing). Then the molecule (electron) passes upward overcoming friction (resistance) and inertia (inductive reactance) and finally is stored in the upper chamber (second capacitor). Because of the sudden shift in molecules (electrons) from the lower chamber (first capacitor) to the upper chamber (second capacitor), the pressure drop at the orifice (voltage across the tube) is reduced until bubble formation (tube firing) stops. Molecules (electrons) stored in the upper chamber (second capacitor) trickle off to the atmosphere (ground). This explanation is in terms of a type 2 bubbler, but the explanations for types 1 and 3 follow with only a few modifications. No net current flows directly from the first capacitor to the second.

McLachlan (9) shows that the capacitance of a volume of gas is proportional to $\frac{V}{p\gamma}$. Hence, in a bubbler operating at nearly constant pressure the capacitance of a chamber is proportional to its volume.

If, in the analogue shown in Figure 6, the capacitors are large and the critical stopping potential is only a few percent less than the critical starting potential, the current through the diode (orifice) may be represented by Figure 7. Since Q_i is analogous to current, the volume of a bubble, v, is equal to TQ_i. On the other hand

$$v = \frac{Q}{f} \tag{2}$$

so that

$$f = \frac{Q}{TQ_i} = \frac{1}{T'} \tag{3}$$

T does not vary with Q; on the other hand, Q_i (and hence v) does vary with Q.

Figure 8 shows the history of the potential difference across the diode. The potential increase during the buildup period and the decrease during discharge are nearly linear. If a type 1 apparatus is used, one chamber is always at the same pressure, and Figure 8 may be regarded as also showing the pressure history of the lower chamber. The ordinates in Figure 8 then vary between the starting pressure and the stopping pressure. This variation is due to the change in inventory of the lower chamber. This transient inventory may be expressed as a gas volume measured at some standard pressure. If it is measured at the orifice pressure, its history is shown in Figure 9. The ordinate is called *excess volume* and is calculated from Figure 8 by multiplying p_{xs} by V_L/p_o. The maximum ordinate of Figure 9 may be evaluated when bubble formation is studied at small values of Q. At these low gas flow rates only the

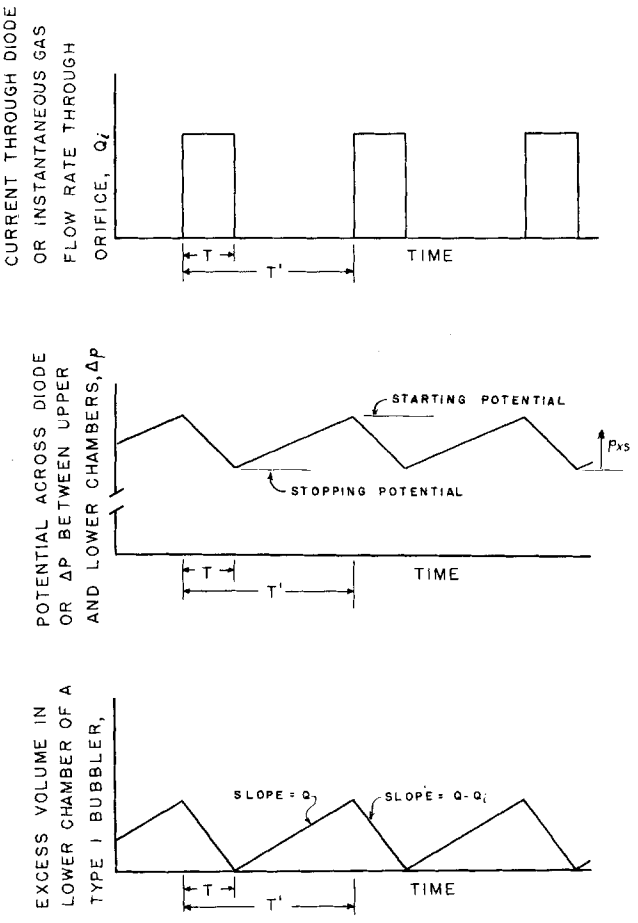

Top: Fig. 7. History of gas flow through the bubbler or of current flow through the diode. Center: Fig. 8. History of potential difference: pressure drop across the orifice or electrical potential at the diode. Bottom: Fig. 9. History of excess volume.

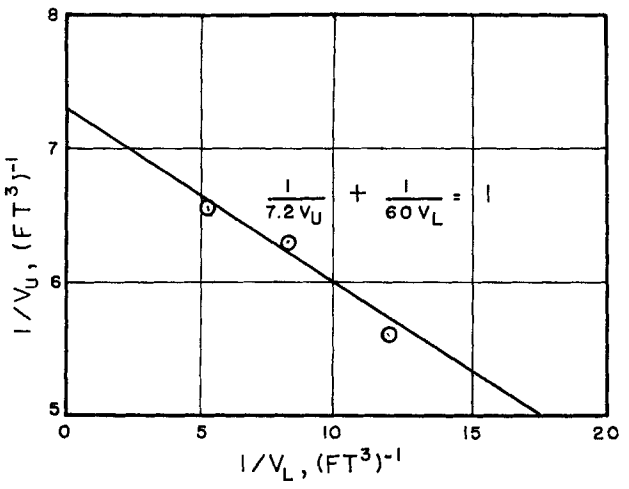

Fig. 10. Relation between chamber volumes giving frequency curve B, Figure 4.

excess volume is released in the form of a bubble; hence the maximum ordinate is labeled v_o, the bubble volume at small values of Q. At greater values of Q, a bubble releases the excess volume plus that volume of gas added to the lower chamber when the bubble is being formed; that is, $v_o + TQ$. The maximum ordinate of Figure 9 is related directly to the potentials given in Figure 8, and hence is a potential and independent of Q. The slopes of Figure 9 for the type 1 apparatus represent the rate of change of volumetric inventory of the lower chamber. During the buildup period the rate of change of inventory is Q; hence

$$Q = \frac{v_o}{T' - T} \tag{4}$$

During the bubble formation period the rate of change of inventory is $Q - Q_i$; hence

$$Q - Q_i = \frac{-v_o}{T} \tag{5}$$

When Equations 3 and 5 or Equations 3 and 4 are combined, the frequency becomes

$$f = \frac{Q}{TQ + v_o} \tag{6}$$

T was measured by the use of high-speed movies. For the conditions that produced curve B in Figure 4, T was 0.067 sec.; v_o was found when the ratio of Q to f was taken at low values of Q (or f). Its value in this particular case was 7×10^{-5} cu. ft. These values of T and v_o were substituted into Equation 6 and then plotted in Figure 4 as curve C. Equation 6 could be made to coincide with curve B if $v_o = 7 \times 10^{-5}$ cu. ft. and $T = 0.05$ sec. Thus a reduction of 25% in the measured value of T resulted in an excellent fit of the data. Only two pieces of information are needed to use Equation 6: the volume of a bubble formed at small values of Q and the formation time of a bubble.

When one refers to the electrical analogue it is apparent that the capacitors are in series and hence may be combined into one. Capacitances in series are combined by addition of their reciprocals. If the electrical analogy is correct, the capacitance relation of McLachlan (9) may be used:

$$\text{Capacitance} \propto \frac{V}{p\gamma} = DV \tag{7}$$

When it is assumed that p and γ do not vary appreciably within the bubbler, reciprocals of chamber volumes may be added with the direct addition empirically modified because of fluid nonlinearities. An equation results relating those chamber volumes that give identical bubble frequency curves:

$$\frac{C}{V_U} + \frac{E}{V_L} = 1 \tag{8}$$

For the condition used here C was larger than E.

To find the values of C and E for those runs that form curve B in Figure 4, $1/V_U$ is plotted vs. $1/V_L$ as shown in Figure 10. From Equation 8, $C = 0.139$ cu. ft. and $E = 0.0167$ cu. ft. From these values and Equation 8, all sets of V_U and V_L that give the frequency curve B may be predicted. Also, when $V_L = \infty$ (type 3 bubbler), $V_U = C$; when $V_U = \infty$ (type 1 bubbler), $V_L = E$. Thus C and E may be evaluated by finding V_L in a type 1 bubbler and V_U in a type 3 bubbler that give identical frequency curves. These values of C and E will allow prediction of all sets of V_U and V_L in a type 2 bubbler that will also give this same frequency curve. If the desired frequency curve is to be produced, V_U may not be less than C, and V_L may not be less than E.

The glass orifice plate used to obtain curve B in Figure 4 was cleaned so that the contact angle was only 30 deg. Again three sets of upper and lower chamber volumes were used, and two of the sets were chosen by trial and error. Figure 11 shows the resulting frequency curve. This curve differs from curve B despite the fact that one set of chamber volumes was the same in both cases. This shows that plate wettability has an effect. When the three sets of V's were plotted as in Figure 10, $C = 0.0703$ cu. ft. and $E = 0.046$ cu. ft.; these values are different from the previous case. As a further check, the apparatus was converted into a type 1 bubbler with $V_L = 0.046$ cu. ft., and the frequency curve was obtained (7). The apparatus was also modified to a type 3 bubbler and the frequency curve again obtained (11). As can be seen from Figure 11 these last two frequency curves agree well with the predicted curve.

COMPARISON WITH LITERATURE

The literature contains few data which permit additional verification of Equation 8. Frequency-curve data are, however, available for testing Equation 6. Quigley, Johnson, and Harris (10) present frequency data using the liquids water, glycerine, and carbon tetrachloride for several size orifices. In their apparatus $V_U = \infty$. The value of V_L is unspecified, but it appears to be several cubic inches. With their data for a 1/16-in. orifice (runs B, G, M) values of v_o and T were found. For water $v_o = 2.02 \times 10^{-5}$ cu. ft.; for glycerine $v_o = 3.69 \times 10^{-5}$ cu.

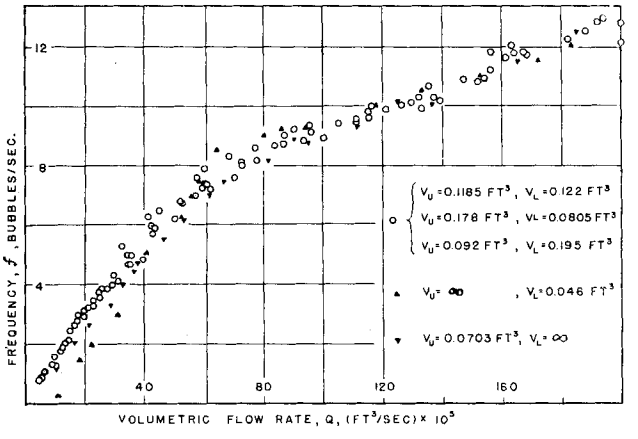

Fig. 11. Frequency-curve duplication. The contact angle is 30 deg.

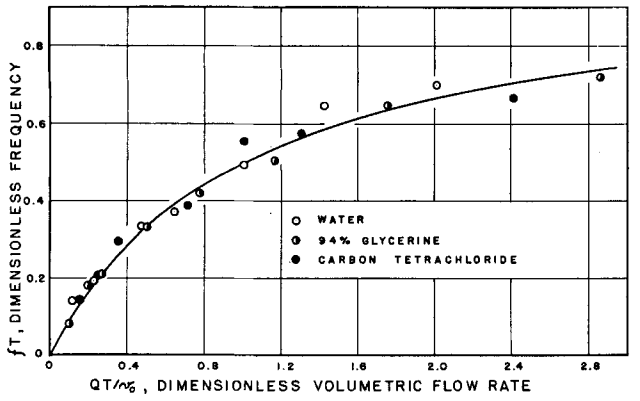

Fig. 12. Frequency curves from Quigley, Johnson, and Harris (*10*) with 1/16 in. orifice.

ft.; for carbon tetrachloride $v_o = 1.74 \times 10^{-5}$ cu. ft. The value of T was 0.024 sec. in all three cases. This suggests that v_o is a strong function of fluid properties, whereas T is a function of the apparatus.

All of these data fit Equation 6 as shown in Figure 12. Here the dimensionless form of the equation is used:

$$fT = \frac{QT/v_o}{1 + QT/v_o} \tag{9}$$

CONCLUSIONS

When the chamber volumes are large and cluster formation is not a factor, the frequency curve is given by an equation of the following form:

$$f = \frac{Q}{A + BQ} \tag{10}$$

The constant A is identified as v_o, the bubble volume at small values of Q. This is a mathematical necessity since the initial slope of Equation 10 is $1/A$, and since in practice v_o may be obtained from the reciprocal of the initial slope of the experimental frequency curve. The constant B equals T, the time for bubble formation. Equating B to T is more difficult. For large values of Q, the frequency according to Equation 10 is $1/B$. For this case the bubbling may be thought of as approaching the condition known as chain bubbling. In chain bubbling the bubbles abut against one another like a chain of pearls. Clearly the frequency then becomes $1/T$, and B equals T. There is conflicting evidence in the literature concerning the existence of chain bubbling. It was not observed in this work, but it still represents a convenient model. With A and B so identified, Equation 10 becomes Equation 6. The T evaluated with high-speed motion pictures was only 33% greater than the value of B obtained empirically from bubble-frequency data. This discrepancy between B and T probably could be eliminated if the wave forms of Figure 7 were altered to have sloping sides. As yet, however, not enough evidence has been collected to warrant such a model change.

Both of the gas spaces above and below the orifice influence the bubble frequency curve. An infinite number of sets of upper and lower chamber volumes give identical bubble-frequency curves. The volumes in such a family are related by Equation 8. In this equation C is larger than E over the range of conditions tested. If gas pressure or properties change as well as chamber volumes, Equation 8 may be extended to give

$$\frac{C_1}{V_{U2}} + \frac{E_1}{V_{L2}} = \frac{\gamma_1 p_1}{\gamma_2 p_2} \tag{11}$$

Here the subscript 1 refers to the conditions under which C and E were determined, and subscript 2 refers to a new condition in which pressure and gas properties were altered. Equation 11 is untested.

The effect of orifice-plate wettability was definite, but unfortunately no general rule may be made as to its effect. The change in frequency due to plate wettability seems to be less than 10%.

ACKNOWLEDGMENT

The authors wish to thank Texaco Incorporated and the Allied Chemical Company for their financial support.

NOTATION

A = constant in Equation 10, cu. ft.
B = constant in Equation 10, sec.
C = constant in Equation 8, cu. ft.
D = constant in Equation 7, sq. ft./lb.
d = orifice diameter, cm.
E = constant in Equation 8, cu. ft.
f = bubble frequency, sec.$^{-1}$
g = gravitational acceleration, cm./sec.^{2}
i = current
p = pressure, lb./sq. ft.
p_o = pressure at orifice, lb./sq. ft.
p_{xs} = excess pressure, defined in Figure 9, lb./sq. ft.
Q = time-averaged volumetric flow rate, cu. ft./sec.
Q_i = instantaneous volumetric flow rate through orifice, cu. ft./sec.
T = bubble formation time, sec.
T' = period of bubble cycle = $1/f$, sec.
V = volume, cu. ft.
V_U = upper chamber volume, cu. ft.
V_L = lower chamber volume, cu. ft.
v = bubble volume, cu. ft.
v_o = bubble volume for very small values of Q, cu. ft.
v_{xs} = excess volume = $p_{xs} V_L/p_o$, cu. ft.
w = weep rate, cc./sec.
γ = ratio of specific heats
σ = surface tension, dynes/cm.
ρ_G = density of gas, g./cc.
ρ_L = density of liquid, g./cc.

LITERATURE CITED

1. Benzing, R. J., and J. E. Meyers, *Ind. Eng. Chem.*, **47**, 2087-2090 (1955).
2. Bowman, C. W., and A. I. Johnson, *Can. J. Chem. Eng.*, **40**, 139-147 (1962).
3. Calderbank, P. H., *Trans. Inst. Chem. Engrs. (London)*, **34**, 79-90 (1956).
4. Davidson, Leon, and Erwin Amick, *A.I.Ch.E. Journal*, **2**, 337 (September, 1956).
5. Hughes, R. R., A. E. Handlos, H. D. Evans, and R. E. Maycock, *Chem. Eng. Progr.*, **51**, 557 (1955).
6. Johnson, A. I., D. G. Robinson, and C. P. Michellepis, Paper presented at A.I.Ch.E. meeting (November, 1955).
7 Klingerman, R. H., B.S. thesis, Lehigh Univ., Bethelehem, Pa. (1961).
8. Mahoney, J. F., Ph.D. thesis, Lehigh Univ., Bethlehem, Pa. (1960).
9. McLachlan, N. W., "Theory of Vibrations," p. 9, Dover Publications, New York (1951).
10. Quigley, C. T., A. I. Johnson, and B. L. Harris, *Chem. Eng. Progr. Symposium Ser. No. 16*, **51**, 31-45 (1955).
11. Talucci, J. F., B.S. thesis, Lehigh Univ., Bethlehem, Pa. (1961).
12. Van Krevelen, D. W., and P. J. Hoftijzer, *Chem. Eng. Progr.*, **46**, 29-33 (1950).

Manuscript received Auuust 16, 1961; revision received April 1, 1963; paper accepted April 2, 1963.